Pergamon

Tetrahedron 54 (1998) 165–178

TETRAHEDRON

Topographically Constrained Aromatic α–Aza-Amino Acids. Synthesis, Molecular Structure, and Conformation of Two AzaTic Derivatives

Ines Torrini,[a] Giampiero Pagani Zecchini,[a] Mario Paglialunga Paradisi,[a] Gino Lucente,[a,*] Gaia Mastropietro,[a] Enrico Gavuzzo,[b] Fernando Mazza,[b] and Giorgio Pochetti[b]

[a] Dipartimento di Studi Farmaceutici and Centro di Studio per la Chimica del Farmaco del CNR, Università "La Sapienza", 00185 Roma

[b] Istituto di Strutturistica Chimica CNR, C.P. n. 10, Monterotondo Stazione, 00016 Roma and Dipartimento di Chimica, Università di L'Aquila, 67100 L'Aquila, Italy

Received 26 September 1997; revised 28 October 1997; accepted 30 October 1997

Abstract: 3,4-Dihydro-2(1*H*)-phthalazinecarboxylic acid (azaTic) is a new conformationally restricted analogue of phenylalanine which, due to its α-aza-nature, should allow, in addition to the topographical control typical of the Tic residue, a definite local perturbation of the backbone conformation. Two azaTic models, namely azaTic-NH_2 (2) and MeCO-azaTic-NHMe (5), have been synthesized and their conformation has been determined and compared to that of the related Tic and azaPro models.

INTRODUCTION

In the field of bioactive peptide analogues increasing attention is devoted to conformationally constrained models possessing specific topographical properties. The ultimate purpose of the designers is the realization of a reasonable control on both the backbone (ϕ, ψ) and side chain (χ^1, χ^2) torsion angles of the synthetic ligands. This approach, effectively referred to as "topographical design on a stable template",[1] is bound to provide valuable insights into the nature of bioactive conformations and topology of the receptor binding domains.

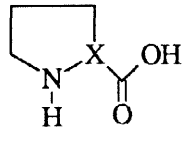

Pro: X = C
azaPro: X = N

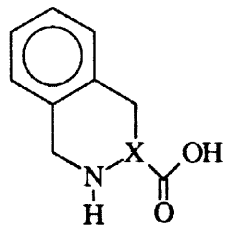

Tic: X = C
azaTic: X = N

A well established example of a synthetic α-amino acid able to limit the backbone flexibility, whilst

0040-4020/98/$19.00
PII: S0040-4020(97)10267-8

maintaining a definite spatial orientation of the side chain, is the tetrahydroisoquinolinecarboxylic acid (Tic).[1-9] The benzylic side chain of this phenylalanine analogue makes part of a 6-membered ring and can only adopt arrangements corresponding to the g^+ (χ^1 = +60°) or g^- (χ^1 = -60°) staggered rotamers; furthermore recent results show that the Tic residue can be easily accomodated into both helical and β-bended structures.[4]

Recently, a new conformationally constrained analogue of the phenylalanine residue has been described;[10,11] this is the 3,4-dihydro-2(1*H*)-phthalazinecarboxylic acid (azaTic) which is the α-aza-analogue of the Tic residue. The azaTic should retain the advantages pertaining to the topographical control which are intrinsic of Tic, introducing at the same time more pronounced and specific effects on the backbone conformation. This expectation is based on the well recognized conformation perturbations induced into pseudopeptides by aza-proline,[12-14] a synthetic α-aza-amino acid which contains an endocyclic hydrazinic fragment analogous to that present in the azaTic residue.

Here we report synthesis and conformation of the two azaTic derivatives azaTic-NH_2 (**2**) and MeCO-azaTic-NHMe (**5**). These two new models have been designed so as to give information on the conformational behaviour of the new α-aza-residue when it is inserted at the *N*-terminal and central position, respectively, of a peptide backbone. Whereas the azaTic residue has been recently inserted into peptide models,[15,16] no data are at the present available on the solid state conformation of azaTic derivatives and, more in general, on the conformational preferences of pseudopeptides containing an α-aza-amino acid residue located at the *N*-terminal position. This latter structural feature deserves attention on the basis of the following considerations: i) the Tic residue adopts different conformations depending upon the *N*-terminal or central location;[1] ii) the hybridation state of the two intracyclic nitrogen atoms of the azaPro residue has been individuated as the main factor which controls the conformational perturbation induced by this residue.[13] Thus, compound **2**, containing a free and an acylated nitrogen atom on the endocyclic hydrazinic fragment, represents a useful model to acquire information on pseudopeptides containing *N*-terminal α-aza-residues.

RESULTS AND DISCUSSION

Chemistry

The carboxamide **2** was obtained starting from benzyl 3,4-dihydro-2(1*H*)-phthalazinecarboxylate[10] which was treated with potassium cyanate and hydrochloric acid in dioxane to give the key intermediate **1** (Scheme 1). Deprotection of **1** by catalytical hydrogenolysis afforded the phthalazine derivative **2**.

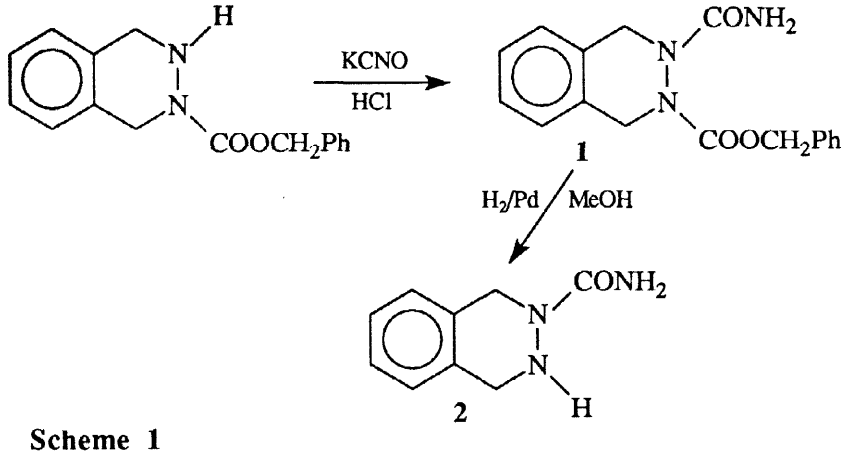

Scheme 1

The *N*-methyl carboxamide **5** was prepared according to the Scheme 2. The key intermediate **3** was obtained by treatment of the protected hydrazine derivative Boc-NH-NH-COMe[17] with α,α'-dibromo-*o*-xylene in the presence of sodium hydride. Deprotection of phthalazine **3** by treatment with trifluoroacetic acid (TFA) followed by acylation with *p*-nitrophenyl chloroformate, afforded the *p*-nitrophenyl ester **4**. Final treatment of **4** with $MeNH_2$ in the presence of 4-(dimethylamino)pyridine (DMAP) afforded the desired compound **5**.

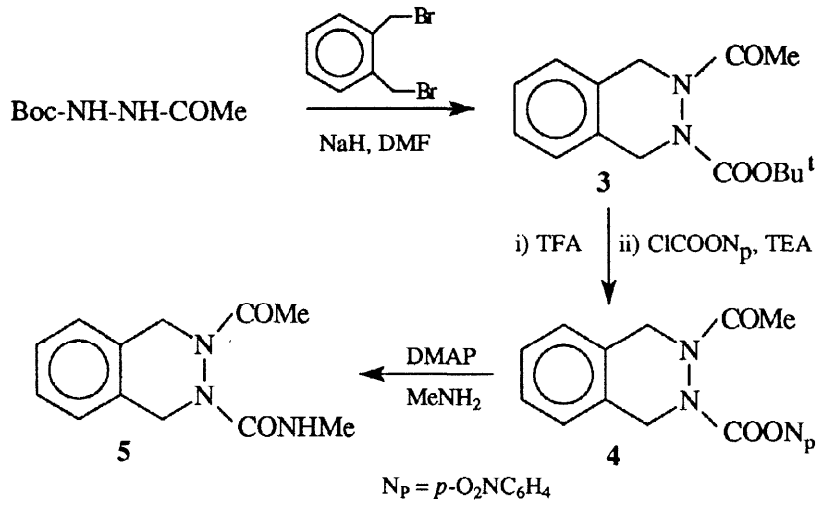

Scheme 2

Molecular Structure of 2 and 5

A perspective view of the molecular conformation of azaTic-NH_2 (**2**) and MeCO-azaTic-NHMe (**5**) together with the atomic numbering scheme is shown in Figure 1. The most relevant torsion angles are reported in Table 1. It is clear from Figure 1 and from the data summarized in Table 2 that the nitrogen atoms of the hydrazinic fragment possess different hybridization states. In particular, compound **2**, which is the model of an *N*-terminal residue, has the free nitrogen atom N_1 with a pronounced sp^3 character whereas the N_1^{α}, bound to the carbonyl group, is nearly planar (sp^2 hybridization). In compound **5**, which is the model of an internal azaTic residue, the N_1 is practically planar (sp^2) whereas the N_1^{α} has a pronounced pyramidal (sp^3) character. The pyramidality of the N_1 in **2** and N_1^{α} in **5** has, as expected, several consequences: two enantiomers for each compound are found in the crystal; the electronic conjugation of the nitrogen lone-pair with the carbonyl π-orbitals is significantly reduced giving rise to remarkable lengthening and shortening of the involved C-N and C-O bond, respectively. Thus (see Table 2), the N_1^{α}-C_1' and C_1'-O_1 bonds in **5** are 1.414 and 1.219 Å as compared with 1.357 and 1.247 Å of compound **2** which possesses a planar (sp^2) N_1^{α} nitrogen atom.

The N-N distance, 1.421 Å in **2** and 1.410 Å in **5**, is less than that observed for the N-C^{α}H in the Tic residue (1.470 Å)[8] and in pyrrolidine ring of Pro (1.48 Å).[13] The N_1-N_1^{α}-C_1' bond angle, which corresponds to the conformationally relevant τ angle of conventional α-amino acids, is 119° in **2** and 116° in **5**; both values are significantly higher than those found in the Tic residues.[4,8]

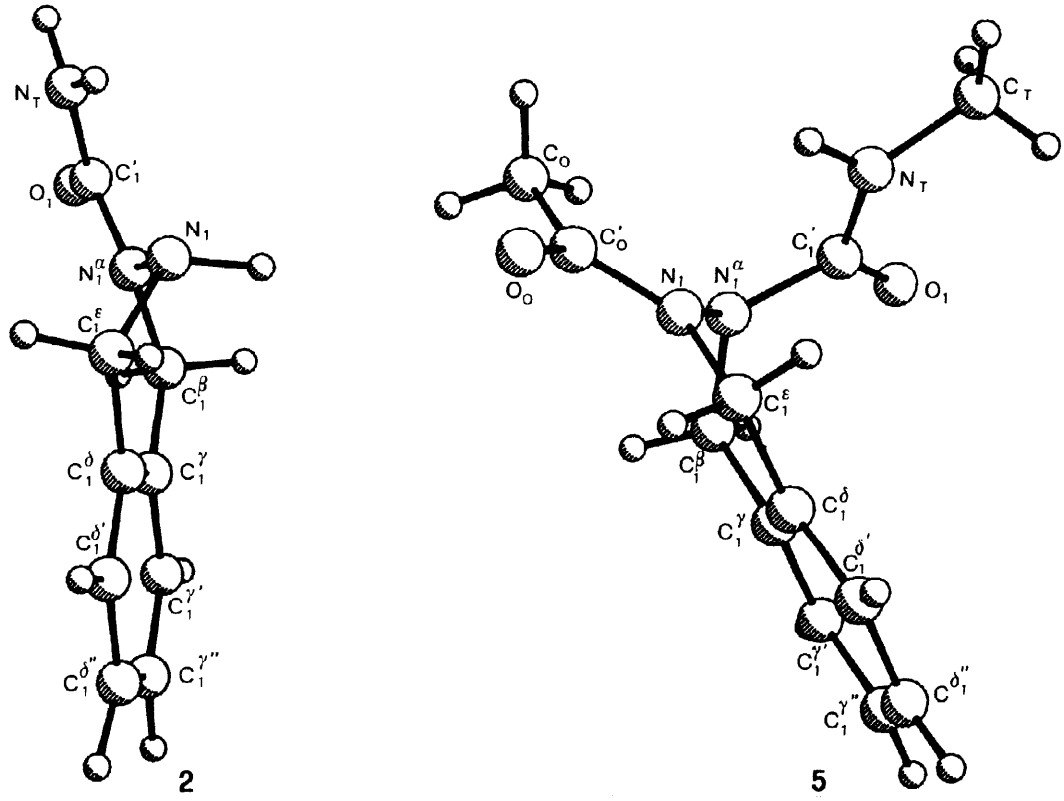

Figure 1. A perspective view of the crystal conformation of the *R* enantiomers **2** and **5.**

The two pseudopeptidic junctions in **5** are fairly planar as it can be deduced by the ω_0 and ω_T torsion angles of Table 1. The *C*-terminal azaTic-NH junction has a *trans* conformation (Figure 1) as usually found in peptides and in the -Tic-Xaa- bonds; conversely, the *N*-terminal -CO-azaTic- link is *cis* configurated. This feature differentiates the azaTic derivative **5** from Tic peptides and evidentiates, at the same time, its analogy with the azaPro-containing models; these latters are, in fact, characterized by a *trans* -azaPro-Xaa- bond preceded by a *cis* -Xaa-azaPro- amide junction.[12-14] As a consequence of this *cisoid* preference, the two carbonyl groups, acylating the endocyclic hydrazinic system, are oriented in opposite direction as usually found in azaPro-containing pseudopeptides. In agreement with models containing the azaPro residue,[12-14] the torsion angle φ (around the N-N bond) of the model **5** is significantly higher than that available to proline or Tic-containing peptides (110-113° against ≈ 90°); furthermore, the (φ, ψ) sequence found in **5** (113°; -25°) is practically identical to that found in the recently studied Z-azaPro-NH-iPr (111°; -23°).[13]

The tetrahydropyridazine ring of azaTicNH$_2$ (**2**) is characterized by the presence of a pseudo two-fold axis bisecting the bonds N_1-$N_1{}^{\alpha}$ and $C_1{}^{\delta}$-$C_1{}^{\gamma}$; this conformation can be described by a half-chair which leaves the N_1 and $N_1{}^{\alpha}$ atoms on opposite side of the other four ring atoms (0.463 Å and 0.240 Å, respectively). In Figure 1 is represented the *R* enantiomer of **2** in the conformation which places the lone pair of the pyramidal nitrogen N_1 in the pseudoequatorial orientation leaving the hydrogen atom pseudoaxial.[18] The conformers

characterized by pseudoaxial lone pair and pseudoequatorial hydrogen atom are less favoured due to steric interference with the pseudoequatorial substituent on the adjacent N_1^{α} atom.

Table 1. Relevant torsion angles (°) of azaTic derivatives **2** and **5** with their e.s.d.'s in parentheses.

		2	**5**
C_0-C_0'-N_1-N_1^{α}	(ω_0)		-5.6(3)
C_0'-N_1-N_1^{α}-C_1'	(φ_1)		113.2(2)
N_1-N_1^{α}-C_1'-N_T	(ψ_T)	-11.3(2)	-24.6(3)
N_1^{α}-C_1'-N_T-C_T	(ω_T)		-174.9(2)
N_1-N_1^{α}-C_1^{β}-C_1^{γ}	(χ_1^1)	43.2(2)	-57.0(2)
N_1^{α}-C_1^{β}-C_1^{γ}-C_1^{δ}	(χ_1^2)	-8.9(2)	26.7
C_1^{β}-C_1^{γ}-C_1^{δ}-C_1^{ε}		-1.7(2)	3.4(3)
N_1-C_1^{ε}-C_1^{δ}-C_1^{γ}		-19.0(2)	-3.8(3)
N_1^{α}-N_1-C_1^{ε}-C_1^{δ}		49.2(2)	-28.6(3)
C_1^{ε}-N_1-N_1^{α}-C_1^{β}		-64.6(2)	60.6(3)
N_1-N_1^{α}-C_1'-O_1		171.0(1)	158.5(2)
C_1^{β}-N_1^{α}-C_1'-N_T		-176.7(2)	-157.9(2)
O_0-C_0'-N_1-N_1^{α}			175.6(2)
N_1-C_1^{ε}-C_1^{δ}-$C_1^{\delta'}$		160.5(2)	175.9(2)
C_1^{ε}-N_1-N_1^{α}-C_1'		129.0(2)	-75.6(2)
C_0-C_0'-N_1-C_1^{ε}			-176.2(2)
C_1^{γ}-C_1^{β}-N_1^{α}-C_1'		-151.1(2)	78.7(2)

The tetrahydropyridazine ring of the azaTic derivative **5** has a different symmetry characterized by a pseudomirror plane passing through the pyramidal N_1^{α} atom and the opposite aromatic C_1^{δ}. A *sofa* conformation[18] with the N_1^{α} displaced 0.653 Å from the plane of the other five ring atom best approximates this six-membered ring arrangement which presents the substituents on the hydrazinic nitrogen atom N_1 and N_1^{α} in the *quasi*-equatorial and *quasi*-axial position, respectively. The *quasi*-axial character of the substituent on N_1^{α} is described by the C_1^{ε}-N_1-N_1^{α}-C_1' torsion angle (Table 1) which is -75.6°; in this conformation the lone pair of the pyramidal N_1^{α} occupies the equatorial position. An analogous disposition, involving the two adjacent substituents on the tetrahydroisoquinolinic system, is found in the case of the Tic containing peptides;[1] as previously noted, this disposition avoids the unfavourable steric interference between 1,2-pseudoequatorial substituents.[1]

Table 2. Relevant geometrical and structural features of azaTic derivatives 2 and 5.

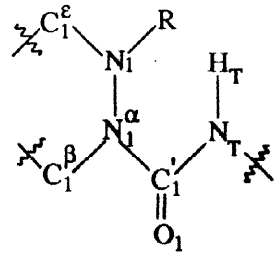

2: R = H

5: R = $C_0' = O_0$

Compound		2	5
Bond lengths (Å)	$C_1^{\varepsilon}-N_1$	1.457	1.464
	$N_1 - C_0'$	—	1.357
	$C_0' - O_0$	—	1.227
	$N_1 - N_1^{\alpha}$	1.421	1.410
	$C_1^{\beta}-N_1^{\alpha}$	1.446	1.465
	$N_1^{\alpha}-C_1'$	1.357	1.414
	$C_1' - O_1$	1.247	1.219
	$C_1' - N_T$	1.327	1.334
N atom hybridization [a]	ΣN_1 (°)	326.6	359.4
	ΔN_1 (Å)	0.444	0.064
	ΣN_1^{α} (°)	358.5	343.5
	ΔN_1^{α} (Å)	0.100	0.340
Short contacts (Å)	$N_1 \cdots N_T$	2.65	2.67
	$N_1 \cdots H_T$	2.26	2.30

[a] Σ N = Sum of the valence angles at the N atom; ΔN = displacement of the N atom from the plane of its three substituents.

The orientation of the benzylic side chain of the *R* enantiomers of **2** and **5** is better represented by the Newman projections of Figure 2 and is described by the χ_1^1 torsion angles (Table 1) which are 43 and -57° for **2** and **5**, respectively. These data show that the β-phenyl ring of **5** adopts the g^- and g^+ staggered conformation in the *R* and *S* enantiomer, respectively. Thus, the internal azaTic residue prefers the rotameric state which locates the aromatic ring between the two bulky substituents bound at the N_1^{α} atom as it is found in pseudopeptide models containing an internal Tic residue.[1,4] In the case of the model **2**, containing a free *N*-terminal nitrogen atom, the benzylic side chain, although bound at a nearly planar nitrogen atom, maintains a χ_1^1 torsion angle fairly similar to that observed in **5** (see Table 1); the sp^2 hybridization of the N_1^{α} atom, however, removes the $N_1^{\alpha}-C_1'$ bond from the aromatic ring as compared with **5**, (see Figure 2) and this is clearly reflected by the C_1^{γ}-C_1^{β}-N_1^{α}-C_1' torsion angle (Table 1) which is 79° in **5** and -151° in **2**. As can be

seen in Fig.s 1 and 2, both the molecules 2 and 5 present a short contact (2: 2.26 Å; 5: 2.30 Å) of the NH···N type between the *C*-terminal N_T-H and the preceding hydrazinic N_1. In both cases the amide hydrogen N_T-H lies directly in the region of space occupied by the lone pair orbital associated with the preceding hydrazinic nitrogen N_1. In particular, the direction of the N_T-H bond in 5 is nearly perpendicular to the lone-pair on the sp^2 N_1 atom. A similar 5-membered ring interaction has been observed in the crystal of Boc-Gly-Gly-NHC_6H_{11}[19] and has been proposed by L. Schäfer *et al.*[20] as an important contribution to the formation and stability of bend type structures in proteins. In the case of pseudopeptides this local folding represents a characteristic conformational feature found in both hydrazino-[21,22] and α-aza-analogues[13,14,23] and has been recently recognized as determining factor in the cyclization reaction leading to cyclo-trihydrazino peptides.[24]

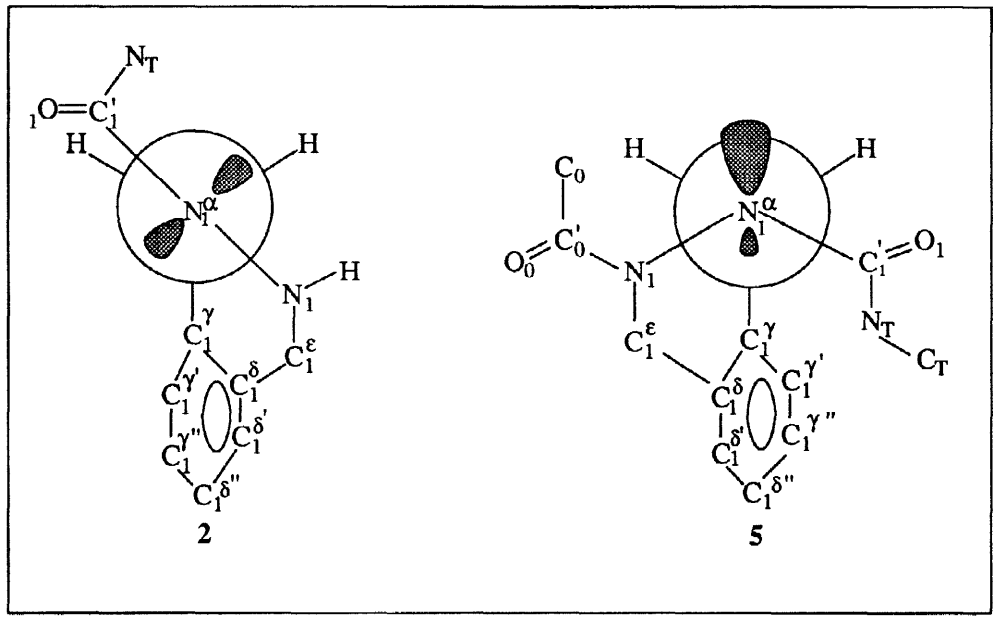

Figure 2. Newman projection along the N_1^{α}-$C_1\beta$ bond for the *R* enantiomers of compound 2 and 5.

Crystal packing

A view of the crystal packing of azaTicNH$_2$ (2) is given in Figure 3. This can be described by an assembly of bilayers extended in the *ab* plane. The structure of a bilayer is mainly stabilized by a network of bifurcated H-bonds that the carbonylic oxygen O_1 forms with the N_1 of glide related molecules and with the N_T of centrosymmetric ones. The contacts that the two intermolecular H-bonds form are as follows: $O_1\cdots N_1$ = 3.022 Å; $O_1\cdots H(N_1)$ = 2.02 Å; $O_1\cdots N_T$ = 2.933 Å; $O_1\cdots H(N_T)$ = 1.99 Å. The van der Waals interactions complete the packing of the bilayers, which give rise to alternating polar and non-polar regions along the *c* direction.

In the crystal of MeCO-azaTic-NHMe (5) (Figure 4), centrosymmetric molecules dimerize by two H-bonds involving the acetyl CO and the amide NH groups. The contacts are as follows: $O_O\cdots N_T$ = 2.850 Å; $O_O\cdots H(N_T)$ = 1.94 Å. Thus, by taking into account the already cited intramolecular short contact $N_T\cdots N_1$, the NH of the residue following the azaTic behaves, in the crystal, as a bifurcated donor[18] with distances $N_T\cdots O$ and $N_T\cdots N_1$ of 2.850 Å and 2.67 Å, respectively. It is worth noting that the lone pair of the pyramidalized

nitrogen atom N_1^{α} does not participate as acceptor site to any H-bonding system. The van der Waals interactions complete the crystal packing where centrosymmetric methyl groups form a contact of 3.645 Å. In the apolar region adjacent aromatic rings stack one on top of another, but charge-transfer interactions can be ruled out since the distance between the mean planes is 3.565 Å.

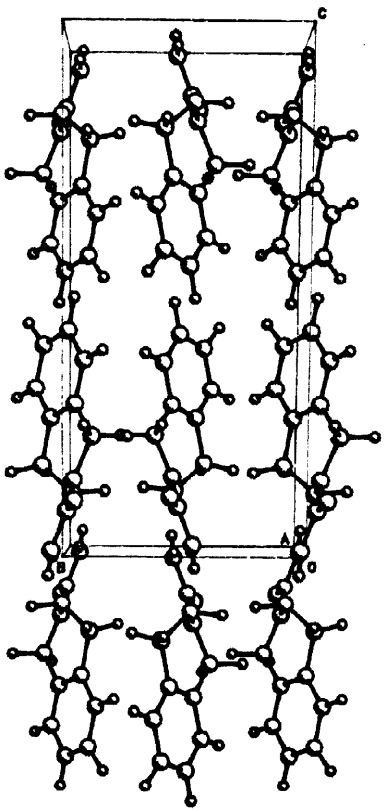

Figure 3. Crystal packing of **2**.

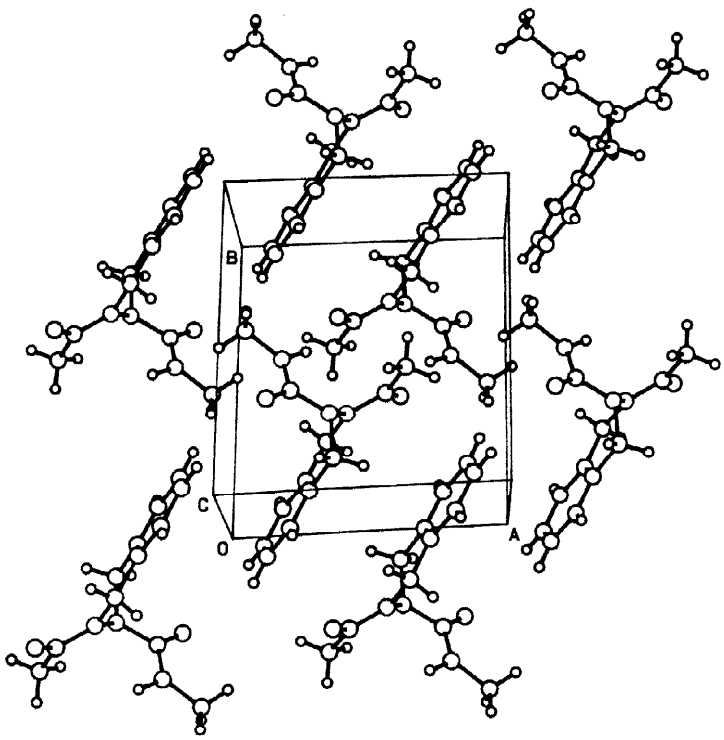

Figure 4. Crystal packing of **5**.

Solution conformation

The ^1H NMR spectrum of the azaTic derivative **5** has been obtained in $CDCl_3$ solution. The CH_3-CO and CH_3-N proton resonances occur at 2.19 (s) and 2.85 δ (d, J = 4.8 Hz), respectively. A characteristic feature of the spectrum of **5** concerns the geminal protons of the two N-CH_2 groups which show significantly large chemical shift difference (Δδ = 1.23 ppm). An analogous behaviour is exhibited by the corresponding protons of the azaPro residue when this occupies the internal position of a peptide backbone.[25] As in the case of the azaPro residue, the resonance pattern of **5** seems related to the diamagnetic anisotropic effect exerted by the two carbonyl groups bonded at the hydrazinic nitrogen atoms, thus suggesting that one of the two protons of each CH_2NCO group is near coplanar with the adjacent carbonyl. However, in the case of the compound under study, the orientation of the aromatic ring towards the geminal protons could also affect the chemical shift.

The involvement of the N_TH group in intramolecular H-bonds has been evaluated on the basis of the chemical shift solvent dependence in a $CDCl_3$-$(CD_3)_2SO$ mixture. In this experiment the NH resonance moves downfield with increasing concentration of $(CD_3)_2SO$ ($\Delta\delta$ = 1.02 ppm), thus the N_TH group is accessible to the solvent as shown in Figure 5. The IR spectrum of the NH stretching region (Figure 6), performed in $CHCl_3$ solution, shows a strong band centered at 3460 cm^{-1} attributable to free NH groups; no significant lower absorptions are observed. Thus the N_TH is free to interact with the solvent, although involved in a short intramolecular contact with the preceding N_1 (see Figure 1 and Table 2). The high deviation from the linearity of the N_T-H···N_1 interaction in addition to the sp^2 hybridization of the acceptor leaves the hydrogen available for an efficient intermolecular interaction; this interpretation is supported by the packing in the crystal which reveals, as above described, a bifurcated interaction (inter- and intra-molecular) of this hydrogen atom. Furthermore, the solvent-exposed nature exhibited by the NH rules out the existence of any significant population of a folded γ-turn conformation stabilized by intramolecular 3-->1 H-bond involving the CH_3-CO as acceptor group.

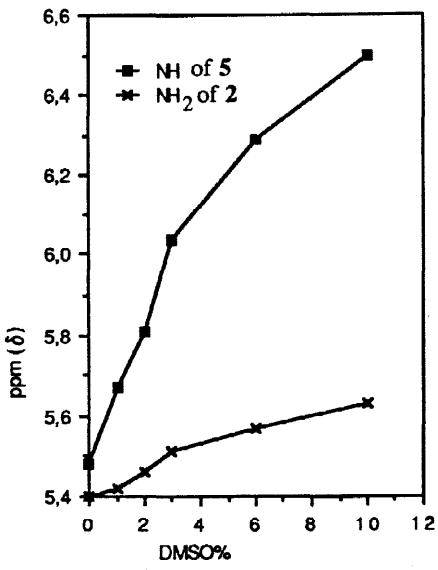

Figure 5. Chemical shift dependence of the NH (5) and NH_2 (2) resonances as a function of the DMSO-d_6 concentration (% v/v) in $CDCl_3$. Peptide concentration 10 mM.

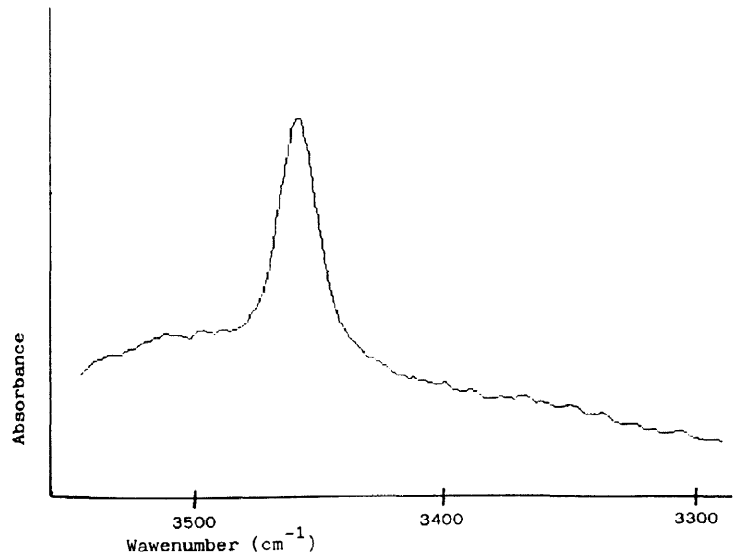

Figure 6. The IR spectrum (NH stretching bands) of 5 in $CHCl_3$. Peptide concentration 1 mM (2mm CsI cell).

In order to gain further information on the solution conformation of 5 two dimensional NMR experiments were carried out. Two medium and one weak NOE signals were detected in the ROESY spectrum of azaTic derivative 5. The two medium effects, observed between the aromatics and the two methylenic protons which resonate at lower field (at 5.41 and 5.46 δ), suggest a different spatial arrangement of the geminal protons of the methylenic groups with respect to the aromatic ring. The weak NOE involving the N-CH_3 group and one of the two CH_2 protons which resonates at higher field is consistent with the axial conformation adopted in the crystal by the CO-NH-CH_3 chain bonded to the tetrahydropyridazine ring.

The absence of any NOE correlation between the $C_1{}^{\varepsilon}H_2$ of the tetrahydropyridazine ring and the methyl protons of the acetyl group C_0H_3 is in accordance with the *cisoidal* configuration of the CH_3CO-AzaTic junction found in the crystal (see Figure 1).

In the ^1H NMR spectrum of carboxamide **2**, performed in $CDCl_3$, the resonance of the CH_2-N-CO group occurs as a singlet at 4.75 δ, while the CH_2-NH resonates as doublet (J = 6.3 Hz) at 4.08 δ. This data indicate that, at variance with the behaviour observed for all the diacylated azaTic derivatives examined (see experimental), the geminal protons of the CH_2-N-CO are in a similar spatial arrangement with respect to carbonyl group.

In the $(CD_3)_2SO$ titration experiment, the amidic NH_2 group is scarcely affected by the change of the solvent composition ($\Delta\delta$ = 0.23 ppm) (Figure 5). This result indicates that, at variance with the N_TH of azaTic model **5**, the NH_2 group of carboxamide **2** is practically solvent inaccessible and presumably involved in an intramolecular H-bond with the preceding N_1. Thus, the sp^3 hybridization of the acceptor nitrogen atom N_1 appears decisive for the stabilization of the 5-membered ring structure in $CDCl_3$ solution.

Conclusion

The above reported results provide the first detailed information on the conformational properties of a novel conformationally constrained analogue of phenylalanine. Similarities and differences with the well known carba-analogue Tic and with the related cyclic α-aza-amino acid azaPro have been evidenced. In particular, the following relevant points can be mentioned: a) a behaviour analogous to that shown by Tic derivatives concerning the rotameric preference of the benzylic side chain; b) a close analogy with the "conservative" structural and conformational features characterizing the azaPro-containing pseudopeptides (i.e.: almost opposite direction of the two carbonyl groups acylating the hydrazinic nitrogen atoms; *cisoid* conformation of the RCO-azaXaa junction; short intramolecular contact of the NH···N type closing a 5-membered ring; definite value of the (φ,ψ) torsion angle sequence).[12-14]

A distinctive structural feature of the azaTic as compared with Tic and azaPro derivatives is represented by the relative spatial orientation of the *N*- and *C*-terminal groups departing from the residue. In fact, in both the Tic and azaPro derivatives these groups are bound to tetrahedral carbon atoms or nitrogen atoms with pronounced pyramidal character. Conversely, in the azaTic derivative **5** - as a consequence of the different constraint imposed by the tetrahydrophthalazine ring - a nitrogen atom is practically planar. This property could significantly influence the nature of the backbone conformational alterations induced by this new residue when inserted into peptides. Studies aimed at gaining further information on this point are in progress in our laboratory.

EXPERIMENTAL

Synthesis

Mps were obtained using a Büchi oil bath apparatus and are uncorrected. IR spectra were recorded on 983 and 16FPC FT-IR Perkin-Elmer spectrophotometers. ^1H NMR spectra were determined in $CDCl_3$ solution with a Varian XL-300 (300 MHz) spectrometer using tetramethylsilane as internal standard. J values are in Hz. A Bruker AM 400 spectrometer operating at 400.13 MHz was used to run two dimensional (2D) spectra. 2D NMR experiments were performed in phase sensitive mode with TPPI phase cycling using 2K of memory for 512 increments. The number of scans was optimized to obtain a satisfactory signal to noise ratio. NOE dipolar correlated 2D spectra in the rotating frame were obtained using the ROESY pulse sequence.[26] The mixing times for the magnetization exchange were 240 ms. Data were processed on a microVAX II computer system using the program TRITON, written by Boelens and Vuister, University of Utrecht, The

Netherlands (courtesy of Prof. R. Kaptein). The FIDs were weighted in both dimensions by a sine-bell apodization function typically shifted by π/3 degrees. The final 2D NMR spectra consisted of 1024 x 1024 data point matrices with a digital resolution of 5 Hz/point. Baseline correction was performed in both dimensions with a 4 term polynomial fit. Column chromatographies were carried out using Merck silica gel 60 (230-400 mesh). TLC and PLC were performed on silica gel Merck 60 F_{254} plates. The drying agent was sodium sulphate. All the reactions were carried out under nitrogen atmosphere.

Benzyl 3-(aminocarbonyl)-3,4-dihydro-2(1*H*)-phthalazinecarboxylate (1)

Following a known procedure,[27] potassium cyanate (81 mg, 1 mmol) was added over 30 min to a solution of benzyl 3,4-dihydro-2(1*H*)-phthalazinecarboxylate[10] (134 mg, 0.5 mmol) and 4 M hydrochloric acid (0.13 ml) in dioxane (1.2 ml). More 4 M hydrochloric acid (0.13 ml) was added and the mixture was stirred at room temperature overnight. After removal of the dioxane *in vacuo*, the solution was extracted with ethyl acetate. The extracts were washed with 5% aq. $NaHCO_3$, brine, and dried. The solvent was evaporated to give a residue which was chromatographed on a silica column (1:40) and eluted with dichloromethane-ether (8:2). Further purification by PLC [dichloromethane-ethyl acetate (1:1) as eluant] afforded the title compound **1** (69 mg, 44%), mp 129.5-130 °C (from ethyl acetate-*n*-hexane); ν_{max} (KBr)/cm^{-1} 3429, 1711, 1680, 1672 and 1601; δ_H 4.30 and 5.24 (2H, A and X of an AX, *J* 16.5, CH_2-N-COO), 4.42 and 5.05 (2H, A and B of an AB, *J* 16.4, CH_2-NCO), 5.17 (2H, s, CH_2-O-CO), 5.47 (2H, s, NH_2), 7.03-7.38 (9H, m, aromatic). Anal. Calcd for $C_{17}H_{17}N_3O_3$: C, 65.58; H, 5.50; N, 13.50. Found: C, 65.70; H, 5.46; N, 13.72.

3,4-Dihydro-2(1*H*)-phthalazinecarboxamide (2)

A solution of compound **1** (96 mg, 0.31 mmol) in dry methanol (10.6 ml) was subjected to catalytic hydrogenolysis, using 5% Pd/C as catalyst (38 mg). After 1 h the catalyst was removed by filtration through sea sand and the solution evaporated under reduced pressure. The pure residue of carboxamide **2** (53 mg, 97%) was crystallized from MeOH, mp 188 °C (decomp.; oil bath heated at 145 °C); ν_{max} (KBr)/cm^{-1} 3422, 3233, 1663, 1597, and 1581; δ_H 3.74 (1H, poorly resolved t, NH), 4.08 (2H, d, *J* = 6.3, C*H*$_2$-NH), 4.75 (2H, s, CH_2-N-CO), 5.40 (2H, br, NH_2), 7.02-7.28 (4H, m, aromatic).

***tert*-Butyl 3-acetyl-3,4-dihydro-2(1*H*)-phthalazinecarboxylate (3)**

Sodium hydride (80% dispersion, 60 mg, 2 mmol) was suspended in dry *N*,*N*-dimethylformamide (DMF) (0.9 ml). After cooling at 0 °C, a solution of Boc-NH-NH-COMe[17] (174 mg, 1 mmol) in DMF (1.8 ml) was added slowly. After stirring at room temperature for 30 min, the mixture was cooled at 0 °C, and a solution of 96% α,α'-dibromo-*o*-xylene (275 mg, 1 mmol) in dry DMF (1 ml) was then added dropwise. Stirring was continued at 0 °C for 5 min and at room temperature for 24 h. The mixture was cooled at 0 °C and the excess of the hydride was decomposed with the minimum amount of ethyl acetate. The solvent was removed *in vacuo* and the residue was taken up with ethyl acetate and washed with water, 20% aq. citric acid, saturated aq. $NaHCO_3$, and brine. The organic solution was dried and evaporated to give a residue which was purified by chromatography on a silica gel column (1:40). Elution with CH_2Cl_2 and CH_2Cl_2-Et_2O (9:1) afforded the acetyl derivative **3** (144 mg, 52%), mp 81-82 °C (from *n*-hexane); ν_{max} (KBr)/cm^{-1} 1710 and 1672; δ_H 1.45 [9 H, s, $C(CH_3)_3$], 2.14 (3 H, s, CH_3-CO), 4.20 and 5.32 (2H, A and X of an AX, *J* 16.5, CH_2-

N-COO), 4.35 and 5.14 (2H, A and X of an AX, *J* 16.1, CH_2-N-CO), 7.10-7.28 (4H, m, aromatic). Anal. Calcd for $C_{15}H_{20}N_2O_3$: C, 65.19; H, 7.30; N, 10.14. Found: C, 65.50; H, 7.60; N, 10.22.

p-Nitrophenyl 3-acetyl-3,4-dihydro-2(1*H*)-phthalazinecarboxylate (4)

The compound **3** (413 mg, 1.475 mmol) was dissolved in a mixture of TFA (0.88 ml) and dry $CHCl_3$ (2.64 ml) and stirred at room temperature for 12 h. The solvent was removed under reduced pressure and the residue was washed several times with dry Et_2O and dried *in vacuo*. To a chilled solution of this crude trifluoroacetate in dry EtOAc (5.9 ml) and triethylamine (TEA) (0.47 ml, 3.39 mmol), a solution of *p*-nitrophenyl chloroformate (357 mg, 1.77 mmol) in EtOAc (2.9 ml) was added during 15 min. The mixture was stirred at 0 °C for 5 min and at 40 °C for 24 h. Ethyl acetate was added in excess and the organic phase was washed with 5% aq. $KHSO_4$, water, saturated aq. Na_2CO_3, and brine. The organic layers were dried and evaporated to give a residue which was chromatographed on a silica gel column (1:40). Elution with *n*-hexane-Et_2O (1:1) afforded the ester **4** (275 mg, 55%) as a solid, homogeneous on TLC, which was not further characterized.

3-Acetyl-3,4-dihydro-*N'*-methyl-2(1*H*)-phthalazinecarboxamide (5)

To a stirred solution of the above active ester **4** (153 mg, 0.45 mmol) and DMAP (14 mg, 0.11 mmol) in dry DMF (2.3 ml) methylamine hydrochloride (30 mg, 0.45 mmol), neutralized with NaOH dissolved in the minimum amount of water, was added dropwise at room temperature. After 6 h the same amount of methylamine was added and the stirring was continued for 19 h. The solvent was evaporated under reduced pressure and the residue partitioned between ethyl acetate and water. The organic phase was washed with 5% aq. $KHSO_4$, water, saturated aq. Na_2CO_3, and brine. After drying and evaporation, the residue was purified by PLC (Et_2O-*n*-hexane, 8:2, 4 runs) to give the carboxamide **5** (93 mg, 89%), mp 139-139.5 °C (from EtOAc-*n*-hexane); ν_{max} (KBr)/cm^{-1} 3307, 1690 and 1659; δ_H 2.19 (3 H, s, CH_3-CO), 2.85 (3H, d, *J* 4.8, CH_3-N), 4.18 and 5.41 (2H, A and X of an AX, *J* 16.6, CH_2-N-CO-NH), 4.23 and 5.46 (2H, A and X of an AX, *J* 16.6, CH_2-N-CO-CH_3), 5.48 (1H, m, NH), 7.07-7.24 (4H, m, aromatic). Anal. Calcd for $C_{12}H_{15}N_3O_2$: C, 61.78; H, 6.48; N, 18.02. Found: C, 62.00; H, 6.66; N, 18.22.

The assignments to two tetrahydrophthalazine CH_2 groups of compounds **1**, **3**, and **5** can be inverted.

X-ray Data Collection and Reduction

Crystals of the aza-analogues **2** and **5** were obtained from methanol and ethyl acetate-*n*-hexane, respectively, by slow evaporation. X-ray data for the two compounds were collected at room temperature on a Rigaku AFC5R diffractometer with graphite monochromated Cu-kα radiation and a 12KW rotating anode generator. Cell constants and the orientation matrix for data collection were obtained from a least-squares fit of the angular settings of 25 carefully centered reflections in the range $40°<2\theta<70°$. The cell parameters, refined on higher angle reflections, are reported on Table 3. Intensity data were collected by the $\omega/2\theta$ scan technique at a variable and appropriate speed to a maximum 2θ of 124°. Stationary background counts were recorded on each side of the reflection. The peak counting time was twice that of the background. Reflections with $I<20\sigma(I)$ were rescanned with an accumulation of counts to improve counting statistics. Out of 1691 (compond **2**) and 2019 (compound **5**) collected reflections, 1564 (**2**) and 1880 (**5**) were unique, 1269 (**2**) and 1559 (**5**) had $I>3\sigma(I)$ and were used in the refinement. The intensities of three standard reflections, measured after every 97 reflections, remained constant throughout data collection indicating crystal and electronic

stability. An empirical absorption correction, based on azimuthal scans of several reflections, was applied resulting in transmission factors ranging from 0.78 to 1.00 (2) and from 0.86 to 1.00 (5). The data were corrected for Lorentz and polarization effects. A correction for secondary extinction was finally applied (coefficient = 6.0×10^{-6} for derivative 2 and 2.3×10^{-4} for 5).

Table 3. Crystal data for compounds 2 and 5.

	2	5		2	5
Empirical formula	$C_9H_{11}N_3O$	$C_{12}H_{15}N_3O_2$	d_c (g/ cm^3)	1.29	1.29
Formula weight	177.2	233.3	Z	4	2
Crystal system	monoclinic	triclinic	F (000)	376	248
a (Å)	7.719 (1)	8.8232 (9)	λ (Cu-Kα) (Å)	1.5418	1.5418
b (Å)	7.384 (2)	10.161 (1)	μ (Cu-Kα) (mm^{-1})	0.7	0.7
c (Å)	16.310 (2)	6.8688 (8)	Crystal size (mm)	0.4x0.4x0.03	0.3x0.4x0.02
α(°)	-	98.445 (9)	$2\vartheta_{max}$ (°)	124	124
β(°)	101.83 (1)	99.053 (9)	R, R_w	0.039, 0.061	0.051, 0.088
γ(°)	-	84.224 (9)	Weighting scheme	$4F_o^2/\sigma^2(F_o^2)$	
V (Å^3)	909.9 (3)	600 (1)	S	2.7	4.1
Space group	$P2_1/a$	$P\bar{1}$	Observations/parameter	10.7	10.1

Structure Solution and Refinement

Both structures were solved by direct methods using the program MITHRIL[28] and successive Fourier maps; the non-H atoms were refined anisotropically by the full matrix least-squares method. The function minimized was Σ w $(|F_o| - |F_c|)^2$ where $w = 4F_o^2/\sigma^2(F_o^2)$. From the final difference Fourier map it was possible to detect all the H-atoms for compound 2, whereas, for derivative 5, only most of them, the remainder being located at the expected positions. All the H-atoms were included in the last structure factor calculation with isotropic thermal parameters deduced from the carrier atoms. The final R and Rw are 0.039 and 0.061 for 2, 0.051 and 0.088 for 5, respectively. The atomic scattering factors were those of Cromer and Mann.[29] Anomalous dispersion effects were taken into account adopting Δf' and Δf'' values of Cromer.[30] Refined parameters with and e.s.d's and a list of structure factors are deposited at the Cambridge Crystallographic Data Centre. All the calculations were performed using TEXSAN[31] crystallographic software package.

REFERENCES

1. Kazmierski, W. M.; Yamamura, H. I.; Hruby, V. J. *J. Am.. Chem.. Soc.* **1991**, *113*, 2275-2283.
2. Kazmierski, W.; Hruby, V. J. *Tetrahedron* **1988**, *44*, 697-710.
3. Kazmierski, W.; Wire, W. S.; Lui, G. K.; Knapp, R. J.; Shook, J. E.; Burks, T. F.; Yamamura, H. I.; Hruby, V. J. *J. Med. Chem.* **1988**, *31*, 2170-2177.

4. Valle, G.; Kazmierski, W. M.; Crisma, M.; Bonora, G. M.; Toniolo, C.; Hruby, V. J. *Int. J. Peptide Protein Res.* **1992**, *40*, 222-232.
5. Salvadori, S.; Bryant, S. D.; Bianchi, C.; Balboni, G.; Scaranari, V.; Attila, M.; Lazarus, L. H. *J. Med. Chem.* **1993**, *36*, 3748-3756.
6. Josien, H.; Lavielle, S.; Brunissen, A.; Saffroy, M.; Torrens, Y.; Beaujouan, J.-C.; Glowinski, J.; Chassaing, G. *J. Med. Chem.* **1994**, *37*, 1586-1601.
7. Sawutz, D. G.; Salvino, J. M.; Seoane, P. R.; Douty, B. D.; Houck, W. T.; Bobko, M. A.; Doleman, M. S.; Dolle, R. E.; Wolfe, H. R. *Biochemistry* **1994**, *33*, 2373-2379.
8. Vitagliano, L.; Zagart, A.; Capasso, S.; Salvadori, S.; Balboni, G. *Acta Cryst.***1994**, *C50*, 1135-1138.
9. Déry, O.; Josien, H.; Grassi, J.; Chassaing, G.; Couraud, J. Y.; Lavielle, S. *Biopolymers* **1996**, *39*, 67-74.
10. Russell, J. R.; Garner, C. D.; Joule, J. A. *J. Chem. Soc., Perkin Trans. 1* **1992**, 409-410.
11. Grobelny, D. W. PCT Int. Appl. WO 93/ 18006 (16/09/93).
12. Lecoq, A.; Boussard, G.; Marraud, M.; Aubry, A. *Tetrahedron Lett.* **1992**, *33*, 5209-5212.
13. Lecoq, A.; Boussard, G.; Marraud, M.; Aubry, A. *Biopolymers* **1993**, *33*, 1051-1059.
14. Zouikri, M.; Boussard, G.; Marraud, M.; Didierjean, C.; Del Duca, V.; Aubry, A. Azaproline: hydrogen bonding network and induced chirality in azaproline-containing peptides in comparison with proline. In *Peptides 1994*, Maia, H. L. S. Ed.; ESCOM: Leiden, 1995; pp. 507-508.
15. Kline, T.; Mueller, L.; Sieber-McMaster, E.; Lau, W. F.; Meyers, C. A. *Int. J. Peptide Protein Res.* **1996**, *47*, 142-147.
16. Pagani Zecchini, G.; Torrini, I.; Paglialunga Paradisi, M.; Lucente, G.; Mastropietro, G.; Spisani, S. *Amino Acids*, in press.
17. Carpino, L. A.; Terry, P. H.; Crowley, P. J. *J. Org. Chem.* **1961**, *26*, 4336-4340.
18. Glusker, J. P.; Lewis, M.; Rossi, M. *Crystal Structure Analysis for Chemists and Biologists*; VCH Publishers, Inc.: New York, 1994; p. 472.
19. Gellman, S. H.; Powell, D. R.; Desper, J. M. *Tetrahedron Lett.* **1992**, *33*, 1963-1964.
20. Scarsdale, J. N.; Van Alsenoy, C.; Klimkowski, V. J.; Schäfer, L.; Momany, F. A. *J. Am. Chem. Soc.* **1983**, *105*, 3438-3445.
21. Lecoq, A.; Marraud, M.; Aubry, A. *Tetrahedron Lett.* **1991**, *32*, 2765-2768.
22. Marraud, M.; Dupont, V.; Grand, V.; Zerkout, S.; Lecoq, A.; Boussard, G.; Vidal, J.; Collet, A.; Aubry, A. *Biopolymers* **1993**, *33*, 1135-1148.
23. André, F.; Boussard, G.; Bayeul, D.; Didierjean, C.; Aubry, A.; Marraud, M. *J. Peptide Res.* **1997**, *49*, 556-562.
24. Carret, S.; Baudy-Floc'h, M.; Robert, A.; Le Grel, P. *Chem. Commun.* **1997**, 1441-1442.
25. Pagani Zecchini, G.; Paglialunga Paradisi, M.; Torrini, I.; Lucente, G.; Mastropietro, G; Paci, M.; Spisani S. *Arch. Pharm. Pharm. Med. Chem.* **1996**, *329*, 517-523.
26. Griesinger, C.; Ernst, R. R. *J. Magn. Reson.* **1987**, *75*, 261-271.
27. Dutta, A. S.; Morley, J. S. *J. Chem. Soc., Perkin Trans. 1* **1975**, 1712-1720.
28. Gilmore, C. J. *J. Appl. Cryst.* **1984**, *17*, 42-46.
29. Cromer, D. T.; Mann, J. B. *Acta Cryst.* **1968**, *A24*, 321-324.
30. *International Tables for X-ray Crystallography*, Vol. IV, Kynoch Press, Birmingham, 1974.
31. TEXSAN *Structure Analysis Package*, Molecular Structure Corporation, 1985.